Transferability of a Conceptual Hydrological Model across different temporal scales and basin sizes

Sheng Sheng[1] , Hua Chen[1*], Fu-Qiang Guo[3], Jie Chen[1], Chong-Yu Xu[2*], Sheng-lian Guo[1]

Abstract Practical application of hydrological models requires parameter transfer, both temporally and spatially, to compensate for the lack of data. In this study, the transferability of parameters is evaluated using a lumped hydrological model called the Xinanjiang model to simulate runoff at different spatiotemporal scales in the Jianxi basin in south-east China and its four sub-basins. The functional relationships are built based on the posterior distribution derived by the Differential Evolution Adaptive Metropolis (DREAM) algorithm to mitigate the effect of parameter uncertainty. The results show that (1) the sensitivity of parameters KE, SM, KI and KG shows obvious temporal characteristics, and the sensitivity of NK and CG shows strong spatial characteristics; (2) most relationships between sensitive parameters and scales are remarkable with goodness-of-fit coefficient higher than 0.9, which has been verified to

Hua Chen

Chua@whu.edu.cn

Chong-Yu Xu

c.y.xu@geo.uio.no

[1] State Key Laboratory of Water Resources and Hydropower Engineering Science, Wuhan University, Wuhan 430072, China

[2] Department of Geosciences, University of Oslo, Oslo, Norway

[3] Fujian Shuikou Power Generation Group Co., LTD, Fujian, China

achieve good performance in the temporal and spatial transfer; (3) the spatial transferability of the model is greatly influenced by the difference between the basin sizes; and (4) those parameters with strong spatial characteristics, such as NK and CG, show obvious impacts on the performance and uncertainty of the model transferred from the larger/smaller to smaller/larger basins.

Keyword Parameter transfer; Bayesian method; Posterior distribution; Conceptual hydrological model; Model uncertainty

1. Introduction

Conceptual rainfall-runoff models, based on the physical concept of hydrological phenomena and empirical formula, can scientifically express the mechanism of the hydrologic cycle and thus have been extensively used for simulating runoff dynamics and the water balance (Liu et al. 2017). To match the model response to historical input-output data, model parameters must be calibrated with observed time-series data to achieve appropriate values (Gupta et al. 1998). However, in practical applications, the time series of available data may be limited due to, for example, an insufficient length of data or missing observations, posing fundamental challenges to model calibration and application (Perrin et al. 2007; Sun et al. 2012). Consequently, attention should be paid to transferring parameters across different temporal and spatial resolutions during hydrological modelling (Melsen et al. 2016).

The temporal and spatial scales of input data play an important role in determining model performance and uncertainty. Bloschl and Sivapalan (1995) reported that natural catchments exhibited a stunning degree of heterogeneity and variability in both spatial and temporal scales, which affect state variables, parameters and inputs during conceptual hydrological modelling. Bruneau et al. (1995) found that the degradation of modelling efficiency was more sensitive to an increase in time step than to an increase in spatial size. The work of Wang et al. (2009) showed that the most accurate simulation results were obtained on the peak discharge and recession part of the hydrograph by using the shortest temporal resolution data, and the effects of the time interval were quite different depending on the response time of parameters.

Despite the consensus that model parameters and performance are strongly dependent on their respective scales, parameters transferred from other calibration domains are used to simulate runoff due to a lack of data. In most cases, temporal transferability of parameters is studied based on the functional relationships established. Bastola and Murphy (2013) found great decreases in the loss of model performance by obtaining model parameters using a linear-scaling-relationship function compared with directly using parameters from another temporal steps. However, the derived relationship of parameter values at different scales was based on optimized behavioral parameters, which ignored the equifinality effect of different parameters. Kavetski et al. (2011) argued that the use of robust numeric and more adequate likelihood functions markedly reduced time scale dependencies and improved the stability of parameters within increasingly complex model structures.

However, on account of the intricate characteristics of basins, the transfer of parameters across spatial scales with a functional relationship remains high uncertainty (Bardossy 2007). Therefore, directly using parameters from another basin to study spatial transferability is more popular. Kumar et al. (2013) showed that model simulations with transferred parameters from coarser to finer scales exhibited great losses in accuracy. Zelelew and Alfredsen (2014) found that parameters integrated from one to six donor catchments evidently improved the model performance at ungauged catchments. Chouaib et al. (2018) found that parameter transfer within homogeneous regions outperformed that from directly using a priori parameters in terms of the decrease in bias and increase in efficiency.

Recently, Jie et al. (2018) established a transformation function according to the regular relationship between the median values of posterior distribution parameters and time steps using the Bayesian method, which was found to have a good capacity for model simulation, and validated the feasibility of transferring parameters across temporal scales. This study is a continuation of the study of Jie et al. (2018), aiming to explore the temporal and spatial transferability of parameters. The objective of this study is to build functional relationships of parameters across temporal and spatial scales based on characteristic data of basins to quantify the effect of the difference in time scales and in basin size on the model performance and uncertainty. The goal is achieved through the following steps: first, the sensitivity of parameters with different temporal scales is analysed in each basin; then, the posterior distributions of sensitive parameters are derived using the Bayesian inference and the Differential Evolution Adaptive Metropolis (DREAM) algorithm; functional relationships are then established and parameters are transferred through temporal scales for validation; finally, parameters are spatially transferred and compared using three schemes to explore the spatial transferability.

2. Material and Methods

2.1 Study area and data

The study area is Jianxi River basin (Qilijie) in south-east China, which is almost the same with Jie et al. (2018). The difference is that an additional four sub-basins in Table 1 are considered in this study (Fig. S1), while only Qilijie basin was considered in Jie et al. (2018). Hourly hydrological data for the period 2009-2015, including precipitation data, pan evaporation data and discharge data, are obtained from the Fujian Hydrology Bureau and Shuikou Reservoir. Then, data series with time intervals of 3, 6, 9, 12 and 24-hours are aggregated from the hourly data above.

<Table 1>

2.2 Xinanjiang Model

The Xinanjiang (XAJ) model, a rainfall-runoff model developed by (Zhao 1992), has been widely used in China and many countries in the world for flood simulation in humid and semi-humid regions (Huo and Liu 2020; Liu et al. 2016; Meng et al. 2016; Yang et al. 2020; Zhang et al. 2019; Zhuo et al. 2016). It is based on the concept of saturation excess runoff mechanism, which means that runoff is not produced until the soil moisture content of the aeration zone reaches field capacity. The XAJ model is composed of 4 main modules, namely, the evaporation, runoff generation, runoff partition, and runoff routing modules (Tian et al. 2013). The model calculation involves 15 parameters, which can be divided into 4 categories according to physical meanings. The structure of the XAJ model and the physical meanings of the range of the model parameters are the same with the previous study conducted by Jie et al. (2018) (Table S1).

2.3 Sobol sensitivity analysis for parameters

The Sobol sensitivity analysis method, proposed by Sobol′ (2001), is a global quantitative sensitivity analysis method based on variance decomposition, of which the key idea is to decompose the total variance of the objective function into the variance of each single parameter and the variance generated by the interaction between parameters (Hall et al. 2005). The method can accurately and quantitatively describe the sensitivity of an independent parameter and the sensitivity due to the interaction between parameters (Nossent et al. 2011). Tang et al. (2007) found that the Sobol method could effectively analyse the parameter sensitivity of the lumped hydrological model and the interaction between parameters. The equations to calculate sensitivity indices in Sobol method are as follows:

$$D = \sum_{i=1}^{n} D_i + \sum_{i=1}^{n-1} \sum_{j=i+1}^{n} D_{i,j} + \cdots + D_{1,2,\cdots n} \tag{1}$$

$$S_{Ti} = 1 - \frac{D_{\sim i}}{D} \tag{2}$$

where D_i, $D_{i,j}$ and $D_{1,2,\cdots n}$ represent the variance produced by the i-th parameter, the i-th and j-th parameter, and the interaction of n parameters; and D and $D_{\sim i}$ indicate the variance generated from all parameters and the remaining parameters other than the i-th parameter; and S_{Ti} is the total sensitivity for the i-th parameter. If S_{Ti} is greater than 0.1, the i-th parameter has a significant sensitivity (Wan et al. 2015).

In this study, apart from the Nash–Sutcliffe efficiency (NSE) adopted in Jie et al. (2018), the relative error of the water balance (RE) is also chosen as an additional objective function to evaluate the sensitivity of the model parameters.

2.4 DREAM algorithm

The Differential Evolution Adaptive Metropolis (DREAM) optimization algorithm proposed by Vrugt et al. (2009) is an adaptive Markov Chain Monte Carlo (MCMC) algorithm which can effectively implement Bayesian theory to estimate the posterior parameter distribution of complex high-dimensional sampling problems (Zahmatkesh et al. 2015). Jie et al. (2018) applied DREAM method to generate multiple parallel Markov chains from different search starting points that can fully traverse the parameter space to search for the global optimal solution, which is used to calculate the posterior distribution of the parameters in this study. The uncertainty intervals of simulated runoff are evaluated using two indexes, including median-NSE and average relative interval length (ARIL) (Jie et al. 2018; Xiong et al. 2009).

2.5 Transformation functions

According to the types of transformation relationships established (linear function, power function), the equations used to transfer parameters across temporal scales are as follows (Bastola and Murphy 2013):

$$\theta' = \theta + K(T' - T) \tag{3}$$

$$\theta' = \left(\frac{T'}{T}\right)^{\beta} \cdot \theta \tag{4}$$

where θ' is the parameter estimated with the modelling time step T'; and T and θ represent the known time step and parameter value; and K and B are scaling factors estimated from the linear and power function relationships based on calibration dataset.

Based on the posterior distribution of the parameters and the characteristics of sub-basins, the functions are defined following equations above to transfer parameters across spatial scales at same temporal scale:

$$Z' = Z + \mu_1(S' - S) + \mu_2(\alpha' - \alpha) + \mu_0 \tag{5}$$

In the equation above, Z and Z' represent the known and estimated parameter value at the same temporal scale; S and S', α and α' indicate the areas and rainfall runoff coefficients of basins involved in spatial transform; and μ_0, μ_1 and μ_2 are spatial scaling factors.

3. Results and Discussions

3.1 Parameter sensitivity to varying spatial and temporal scales

The Latin hypercube sampling method (McKay et al. 2000) is used in this paper to extract parameter samples for sensitivity calculation. The total sensitivity of each parameter is calculated under different sampling numbers (1000, 1500, 2000, 3000, 4000, and 5000) at 1-h temporal scale. When the number of samples reaches 3000, the indices of sensitivity are close to stability (Fig. S2). Therefore, for each parameter, 3000 samples are extracted from the feasible domain to compare and analyse the sensitivity in different sub-basins and temporal scales.

The total sensitivities of all parameters at different temporal and spatial scales are plotted in Fig.1. Those parameters are sensitive with the total sensitivities being larger than 0.1. As can be seen from Fig.1, when the objective function is NSE, the sensitive parameters are KE, SM, KI, KG, CI, CG, N and NK. Meanwhile, when the objective function is RE, the sensitivity parameters are KE and CG. These are almost consistent with previous studies (Jie et al. 2018; Song et al. 2013; Zhang et al. 2012). It is reasonable for that NSE reflects the goodness-of-fit of the observed and simulated flow processes and has close relationships with the evapotranspiration, runoff separation and flow routing parameters; while RE mainly reflects the relative error of the water balance between the observed and simulated hydrograph and has closer relationships with the evapotranspiration and flow routing parameters.

<Fig.1>

As can be seen from Fig. 1, for each sub-basin, only KE is sensitive in the four evapotranspiration parameters under both objective functions. The evaporation module uses a three-layer (upper, lower, and deep layer) scheme according to the soil moisture of different layers and rainfall. C is related to the evaporation of lower and deep layer, and its value is affected by X and Y. This indicates they are not easily affected for the stability of the lower and deep layer evaporation, especially in wet zones. It can be seen that C, X, and Y are insensitive at all temporal scales and basins (Fig. S3). Whether the objective function is NSE or RE, KE is sensitive and its sensitivity decreases with the increase of temporal scales as KE is closely related to evaporation in three layers. There is no big difference in the sensitivity of KE among different basins, while its sensitivity is very high when the objective function is RE.

All runoff production parameters are insensitive with NSE and RE adopted as objective functions respectively (Fig.2 and Fig. S4). WM is the areal tension water storage capacity, B and IMP represent the uneven distribution of tension water storage and the proportion of impervious area, respectively. These parameters reflect the physical characteristics of a basin, which are insensitive (Jie et al. 2018; Zhang et al. 2012). Consistent results are derived in this study, and their insensitivities are affected little by the variation of the temporal scales and basin sizes.

The SM, KI and KG retain high sensitivity for NSE, while are insensitive for RE. SM, affected by the time-averaged rainfall data, tends to maintain stable sensitivity at large temporal scales and basin size (Fig.2 and Fig. S5). The sensitivity of SM decreases with the increase of temporal scale except 1-hour in all sub-basins, while the sensitivity of SM is stable in Qilijie basin at all time scales except 1-hour. KI and KG have a direct influence on the size of the interflow and groundwater flow. The sensitivity of KI and KG decreases with the increase of time scale, while the KG gradually becomes insensitive with the increase of time scale in five basins.

Most flow routing parameters, including CI, CG, N and NK, are sensitive in all basins when the objective function is NSE; meanwhile, only CG retains high sensitivity in some basins when the objective function is RE (Fig.2 and Fig. S6). The sensitivity of CI increases as the temporal scales increase in all basins as CI has a great effect on the recession process of runoff, which is enhanced as the temporal scales increase.

There are no obvious differences in the variation of the CI sensitivity among the five basins. To the objective NSE, CG is insensitive in most conditions, while to RE, CG shows great sensitivity in Wuyishan and Xinchang and insensitivity in Qilijie at all temporal scales. CG is the parameter of the recession of groundwater storage and has an impact on the groundwater convergence process. N reflects the regulation ability to the water storage in a basin and is closely related to the convergence time of the basin, its sensitivity increases as the temporal scale increases. And there is no big difference in the variability of the sensitivity of N among the five basins. The sensitivity of NK, which represents flow concentration time, tends to be stable with the increase of temporal scale, while it is lower in small basins than in large ones in this study.

From the above analysis, it can be seen that the sensitivities of SM, KI, KG, CI and N have obvious temporal characteristics when NSE is the objective function. The sensitivity of SM, KI and KG decreases as the temporal scales increase, while the sensitivity of CI and N increases as temporal scales increase. The sensitivity of NK showed strong spatial characteristics, which increases with the increase of basin area. When RE is the objective function, the sensitivity of KE decreases as the temporal scales increase, while the sensitivity of CG decreases with the increase of basin area.

3.2 Parameter posterior distribution among different spatial and temporal scales

The Shuffled Complex Evolution - University of Arizona (SCE-UA) algorithm is employed for parameter calibration at different temporal scales in each basin (Jie et al. 2018). Considering the interaction of parameters and the computational efficiency of the DREAM algorithm, the posterior distribution is only derived from those sensitive parameters with NSE being the objective function, while the values of insensitive parameters are fixed using the mean values of optimized results at all temporal scales.

The box plots of the posterior distribution of sensitive parameters at different temporal scales in each sub-basin are shown in Fig. 2.

<Fig. 2>

As can be seen from Fig. 2, the value and variation of KE with temporal scales perform diversely in different basins. Its value increases in Wuyishan and Shuiji but decreases in other basins. KE controls the total water balance and shows high sensitivity at all scales. As the temporal scale becomes coarser, the 95% confidence interval widths of KE constantly increase. The length of input hydrological series shortens with the data series aggregated to a larger temporal step, which causes the data information loss and increases parameter uncertainty.

For runoff separation parameters, it can be seen that KI and KG are consistently increasing with the increase of temporal scales of each sub-basin. The variation of SM with temporal scale differs in sub-basins, which increases in Xinchang and Qilijie and decreases in Wuyishan, Shuiji, and Jianyang. At the same time, the 95% confidence interval of SM, KI, and KG continuously broadens, which means the temporal scale has an impact on the uncertainty of transferred parameters.

The variation rules of all flow routing parameters with changing temporal scale in different basins coincide with the values decreasing as the temporal scale becomes coarser. According to the physical meanings, the lower the values of CI and CG that relate to the low water part, the longer the water recession. N and NK are instantaneous unit hydrograph parameters, where the low value represents the high peak. Moreover, the 95% confidence interval widths of CI and CG constantly increase, while those of N and NK are unchanged. It can be inferred that the uncertainty of parameters relates to unit hydrograph method is essentially the same at different temporal scales; therefore the transfer can achieve good results.

Compared to the posterior distributions of parameters in Qilijie basin derived by Jie et al. (2018), most results in the five basins in this study are similar to theirs, especially in Qilijie basin, which is completely consistent with their results. However, the posterior distribution of parameters in other sub-basins reflects the following different spatial variation rules: (1) KE and SM show different variation characteristics in different sub-basins; (2) the 95% confidence intervals of most parameters are affected by the sizes of the sub-basins.

3.3 Quantitative relationship of parameters between different basins and temporal scales

Based on the median value of posterior distribution and temporal scale, functions are built according to equations 3 and 4 to transfer parameters across temporal scale in each sub-basin. On the basis of basin characteristic data including area and runoff coefficients, spatial functions are built according to equation 5 to transfer parameters to a specific basin from others from same temporal scale.The goodness-of-fits of temporal and spatial functions for each sub-basin with different coefficients(Table S2, S3 and S4) are shown in Table 2 following the order of watershed area from small to large. For temporal transfer, N and NK present a power function relationship with temporal scales, while others present a linear relationship. Besides, the goodness-of-fits are mainly over 0.95, indicating that remarkable quantitative relationships exist. For spatial transfer, the functional relationships between parameters and basin characteristic data are also obvious with goodness-of-fits mainly higher than 0.9. The effects of transfer functions for KE, SM and CG are slightly worse than others. And there is no big difference in the goodness-of-fits of function of each parameter between different basins. Based on the functions above, the transfer of parameter from another basin and another temporal scale is realized by transferring to same temporal scale using temporal function in another basin first, then transferring across basins using spatial function.

<Table 2>

3.4 Parameter transferability from different temporal scales in five basins

The transformed parameters from other temporal and spatial scales based on the functions above are used in the Xinanjiang model to simulate runoff with NSE as an evaluation index and the results are shown in Fig. 3. For each temporal scale, the median value of NSE using posterior distribution parameters from itself is higher than those using parameters transferred from others. Besides, the larger the scale gap of the transition, the more obvious the loss in NSE. Meanwhile, the 95% confidence interval of model performance widens and uncertainty increases when parameters are transferred from a larger temporal scale, which is consistent with the results of Jie et al. (2018). Besides, as the size of the sub-basin increases, the accuracy of simulation results using posterior distribution parameters and transferred ones at different temporal scales gradually improves. This is in line with the analysis of Merz et al. (2009) on the effect of the basin scale on the model performance who found modeling large basins is easier to get good results than for small ones. More precipitation gauges are contained in larger basins, thus the error of average areal rainfall, the driving data in XAJ model, is relatively smaller, which helps achieve higher accuracy in runoff simulations.

<Fig. 4>

3.5 Parameter transferability from different spatial scales

By using the derived spatial and temporal transfer functions, transfer parameters from another spatial and temporal scale are done according to the following situation: (1) transfer from large basins to small basins; (2) transfer from small basins to large basins; (3) transfer between sub-basins of the similar size. Their results are shown in Fig.4.

<Fig. 4>

(1) Transfer from large basins to small basins

To verify the performance of the parameters transferred from large basins to small basins, 4 cases (Jianyang-Wuyishan; Qilijie-Jianyang; Qilijie-Shuiji; Qilijie-Wuyishan) are adopted, whose performance is shown in Fig.4(a). In the first case, the loss in the median value of NSE is around 0.025 except at 9 and 12-hour scales. In middle two cases, the loss of spatial transfer reaches 0.1 at 24-hour scale and remains around 0.05 at others. In the last case, the model loss maintains 0.1 at small temporal scales, including 1, 3 and 6-hour and decreases at 9, 12 and 24-hour scales. It can be found that the median values of NSE (Qilijie-Wuyishan) are lower than those (Jianyang-Wuyishan) at most temporal scales. This indicates that when the parameters of a larger basin are transferred to a small basin, the transferability of the model may decrease more, which will lead to the worse performance of transferred model. Besides, the loss caused by spatial transfer decreases when temporal scale increases from 1 hour to 12-hour.

(2) Transfer from small basins to large basins

In this situation, there are also 4 cases (Wuyishan-Jianyang; Jianyang-Qilijie; Shuiji-Qilijie; Wuyishan-Qilijie) adopted for comparison and the results are displayed in Fig.4 (b). In the first case, the loss of the median NSE through spatial transfer is close to 0.025 at 24-hour scale and around 0.01 at others. In the second case, the loss is commonly around 0.02 except at 24-hour scale. The model loss in third case is reaching 0.025 at each temporal scale. In the last case, the loss is around 0.05 at sub-daily scales and decreases to 0.01 at daily scale. It can be found that the loss of NSE increases with the increase of the difference between the basin sizes at most temporal scales when transferred from small basin to large basin.

(3) Transfer between sub-basins of the similar size

In this situation, parameters are transferred between similarly sized basins, Jianyang, Shuiji and Xinchang sub-basins, and their performances are shown in Fig. 4(c). Each row represents the result of parameters transferred from other two basins to a specific basin. The model performance transferred from Xinchang is worse than that transferred from Shuiji in the first row, which is more obvious at 1 and 3-hour scales. In the second row, the loss in both cases in Xinchang at each temporal scale is around 0.05 and the width of 95% intervals of NSE is similar. The only difference is that at 1 and 3-hour scales, the model loss caused by parameters transferred from Shuiji from coarse temporal scales is smaller than from Jianyang. In the third row, the loss in model performance in Shuiji is close to 0.05 at each temporal scale and slightly decreases when the temporal scale becomes coarser from 1-hour to 12-hour. In general, the model losses caused by transferring parameters among similar sized basins are ≤ 0.05 at most temporal scales, and little difference exists between the 95% intervals of NSE, thus the result of spatial parameter transfer can be effective for runoff simulation.

(4) Simulation uncertainty of runoff process based on above three situations

To more intuitively compare the simulation uncertainty of the runoff process using parameters transferred from different temporal scales and different basins, three typical floods, including P = 80%, 50% and 1% floods (P is the flood frequency), are selected based on the frequency analysis of 200 flood events, their median-NSE and ARIL are shown in Table 3.

It can be seen from Table 3 that as the frequency of the flood becomes lower, the median-NSE increases and the ARIL decreases, which indicates a better match with the observed runoff and less uncertainty in model performance. The reason is that the observation error of rainfall and flow data is relatively smaller during heavy rainfall periods, helping to improve the simulation accuracy and reduce the simulation uncertainty. When parameters transferred from a large basin to a small basin, the calculated peak times delayed a bit compared to posterior parameters (Fig. S7), which is mainly caused by the longer concentration time in the larger basin. The difference becomes more apparent as the scale gap in basins sizes becomes larger and the error in the simulation of peak value raises. When parameters are transferred from a small basin to a large basin, the peak current time shifts forward while the flood peak becomes smaller (Fig. S8). Moreover, the greater the difference in basin size, the more obvious this phenomenon becomes. The change rule of peak occurring time is opposite to the previous situation due to the effect of parameters and basins sizes. When parameters transferred between basins with similar sizes, more uncertainty is observed in the recession of flood simulation by transferred parameters compared to posterior ones (Fig. S9). It can be seen from Fig.2 that there exists obvious differences in posterior distribution of CG between Jianyang and other two basins, which may lead to the error in recession calculation through spatial transfer. Furthermore, the performance by using parameters from Shuiji is better than that from Xinchang, especially in the simulation of peak (Table 3 and Fig. S9), the reason is that Shuiji is geographically closer and more similar in aspects of slope and land use to Jianyang than Xinchang according to Table 1.

4. Conclusions

The sensitivity and transferability of hydrological model parameters across different temporal and spatial scales are discussed in this study. The Xinanjiang model is applied to the Jianxi basin and its sub-basins at temporal scales of 1, 3, 6, 9, 12 and

24-hour for sensitivity analysis of model parameters. Functional relationships are established and validated for several temporal and spatial scales based on the derived posterior distribution parameters. The conclusions drawn are as follows:

(1) Some parameters' sensitivities show obvious temporal characteristics. The sensitivity of KE, SM, KI and KG decreases with the increase of temporal scales, while the sensitivity of CI and N increases as temporal scales increase. The sensitivity of NK and CG shows strong spatial characteristics, for example the sensitivity of NK increases as the basin area increases, while the sensitivity of CG decreases with the increase of basin area.

(2) Functional relationships between parameters and temporal scales are built with goodness-of-fit coefficient higher than 0.95 and verified to perform well in runoff simulation with a little loss in model performance and an increase in uncertainty when transferring from coarser scales to finer scales. Larger flow events have relatively smaller uncertainty at different temporal and spatial scales.

(3) The spatial transfer function built based on basin characteristic data are remarkable with most goodness-of-fit coefficient higher than 0.9, the effect of which is greatly influenced by the difference between the basin sizes, and the greater differences between the transferred basins sizes tend to lead to the larger loss of NSE for the simulation by using transferred parameters.

(4) Those parameters with strong spatial characteristics, such as NK and CG, show obvious impacts on the performance of the model transferred from larger/smaller to smaller/larger basins. NK, the concentration time of basin, has a great influence on the peak occurring time of the simulation and CG may increase the uncertainty of flood recession when it is transferred between catchments with different sizes.

However, there are also some limitations in this study. The uncertainty in parameters and the model increases when parameters are transferred from coarser to finer scales, thus more work should be done in future to provide a parameter adjustment procedure to reduce model uncertainty during transfer across scales. For spatial transferability, only five basins are considered, which leads to the conclusions may not be representative. More basins with different characteristics and types should be selected in future study. As only one lumped model, Xinanjiang model, is considered in this study, the conclusions cannot be generalised. Therefore, more using hydrological models will be helpful to enrich the spatial and temporal transferability study for hydrological modelling.

Acknowledgements This study is supported by the National Natural Science Fund of China (51539009).

Reference

Bardossy A (2007) Calibration of hydrological model parameters for ungauged catchments. Hydrol Earth Syst Sci 11:703-710 doi:10.5194/hess-11-703-2007

Bastola S, Murphy C (2013) Sensitivity of the performance of a conceptual rainfall-runoff model to the temporal sampling of calibration data. Hydrol Res 44:484-494 doi:10.2166/nh.2012.061

Bloschl G, Sivapalan M (1995) SCALE ISSUES IN HYDROLOGICAL MODELING - A REVIEW. Hydrol Process 9:251-290 doi:10.1002/hyp.3360090305

Bruneau P, Gascuelodoux C, Robin P, Merot P, Beven K (1995) Sensitivity to space and time resolution of a hydrological model using digital elevation data. Hydrol Process 9:69-81 doi:10.1002/hyp.3360090107

Chouaib W, Alila Y, Caldwell PV (2018) Parameter transferability within homogeneous regions and comparisons with predictions from a priori parameters in the eastern United States. J Hydrol 560:24-38 doi:10.1016/j.jhydrol.2018.03.018

Gupta HV, Sorooshian S, Yapo PO (1998) Toward improved calibration of hydrologic models: Multiple and noncommensurable measures of information. Water Resour Res 34:751-763 doi:10.1029/97wr03495

Hall JW, Tarantola S, Bates PD, Horritt MS (2005) Distributed sensitivity analysis of flood inundation model calibration. J Hydraul Eng-ASCE 131:117-126 doi:10.1061/(asce)0733-

9429(2005)131:2(117)

Huo J, Liu L (2020) Evaluation Method of Multiobjective Functions’ Combination and Its Application in Hydrological Model Evaluation. Comput Intel Neurosc 2020:8594727 doi:10.1155/2020/8594727

Jie MX et al. (2018) Transferability of Conceptual Hydrological Models Across Temporal Resolutions: Approach and Application. Water Resour Manag 32:1367-1381 doi:10.1007/s11269-017-1874-4

Kavetski D, Fenicia F, Clark MP (2011) Impact of temporal data resolution on parameter inference and model identification in conceptual hydrological modeling: Insights from an experimental catchment. Water Resour Res 47:W05501 doi:10.1029/2010wr009525

Kumar R, Samaniego L, Attinger S (2013) Implications of distributed hydrologic model parameterization on water fluxes at multiple scales and locations. Water Resour Res 49:360-379 doi:10.1029/2012wr012195

Liu YR, Li YP, Huang GH, Zhang JL, Fan YR (2017) A Bayesian-based multilevel factorial analysis method for analyzing parameter uncertainty of hydrological model. J Hydrol 553:750-762 doi:10.1016/j.jhydrol.2017.08.048

Liu Z, Guo S, Zhang H, Liu D, Yang G (2016) Comparative Study of Three Updating Procedures for Real-Time Flood Forecasting. Water Resour Manag 30:2111-2126 doi:10.1007/s11269-016-1275-0

McKay MD, Beckman RJ, Conover WJ (2000) A comparison of three methods for selecting values of input variables in the analysis of output from a computer code. Technometrics 42:55-61 doi:10.1080/00401706.1979.10489755

Melsen L, Teuling A, Torfs P, Zappa M, Mizukami N, Clark M, Uijlenhoet R (2016) Representation of spatial and temporal variability in large-domain hydrological models: case study for a mesoscale pre-Alpine basin. Hydrol Earth Syst Sci 20:2207-2226 doi:10.5194/hess-20-2207-2016

Meng S, Xie X, Yu X (2016) Tracing Temporal Changes of Model Parameters in Rainfall-Runoff Modeling via a Real-Time Data Assimilation. Water 8:19 doi:10.3390/w8010019

Merz R, Parajka J, Bloschl G (2009) Scale effects in conceptual hydrological modeling. Water Resour Res 45:W09405 doi:10.1029/2009WR007872

Nossent J, Elsen P, Bauwens W (2011) Sobol' sensitivity analysis of a complex environmental model. Environ Modell Softw 26:1515-1525 doi:10.1016/j.envsoft.2011.08.010

Perrin C, Oudin L, Andreassian V, Rojas-Serna C, Michel C, Mathevet T (2007) Impact of limited streamflow data on the efficiency and the parameters of rainfall-runoff models. Hydrolog Sci J 52:131-151 doi:10.1623/hysj.52.1.131

Sobol′ IM (2001) Global sensitivity indices for nonlinear mathematical models and their Monte

Carlo estimates. Math Comput Simulat 55:271-280 doi:10.1016/S0378-4754(00)00270-6

Song X, Kong F, Zhan C, Han J, Zhang X, engineering (2013) Parameter identification and global sensitivity analysis of Xin'anjiang model using meta-modeling approach. Water Sci Eng 6:1-17 doi:10.3882/j.issn.1674-2370.2013.01.001

Sun WC, Ishidaira H, Bastola S (2012) Calibration of hydrological models in ungauged basins based on satellite radar altimetry observations of river water level. Hydrol Process 26:3524-3537 doi:10.1002/hyp.8429

Tang Y, Reed P, Wagener T, van Werkhoven K (2007) Comparing sensitivity analysis methods to advance lumped watershed model identification and evaluation. Hydrol Earth Syst Sci 11:793-817 doi:10.5194/hess-11-793-2007

Tian Y, Xu Y-P, Zhang X-J (2013) Assessment of Climate Change Impacts on River High Flows through Comparative Use of GR4J, HBV and Xinanjiang Models. Water Resour Manag 27:2871-2888 doi:10.1007/s11269-013-0321-4

Vrugt JA, ter Braak CJF, Diks CGH, Robinson BA, Hyman JM, Higdon D (2009) Accelerating Markov Chain Monte Carlo Simulation by Differential Evolution with Self-Adaptive Randomized Subspace Sampling. Int J Nonlinear Sci Numer Simul 10:273-290 doi:10.1515/ijnsns.2009.10.3.273

Wan H, Xia J, Zhang L, She D, Xiao Y, Zou L (2015) Sensitivity and Interaction Analysis Based on Sobol’ Method and Its Application in a Distributed Flood Forecasting Model. Water 7:2924-2951 doi:10.3390/w7062924

Wang Y, He B, Takase K (2009) Effects of temporal resolution on hydrological model parameters and its impact on prediction of river discharge. Hydrolog Sci J 54:886-898 doi:10.1623/hysj.54.5.886

Xiong L, Wan M, Wei X, Oconnor KM (2009) Indices for assessing the prediction bounds of hydrological models and application by generalised likelihood uncertainty estimation. Hydrolog Sci J 54:852-871 doi:10.1623/hysj.54.5.852

Yang X, Magnusson J, Huang S, Beldring S, Xu C-Y (2020) Dependence of regionalization methods on the complexity of hydrological models in multiple climatic regions. J Hydrol 582:124357 doi:10.1016/j.jhydrol.2019.124357

Zahmatkesh Z, Karamouz M, Nazif S (2015) Uncertainty based modeling of rainfall-runoff: Combined differential evolution adaptive Metropolis (DREAM) and K-means clustering. Adv Water Resour 83:405-420 doi:10.1016/j.advwatres.2015.06.012

Zelelew MB, Alfredsen K (2014) Transferability of hydrological model parameter spaces in the estimation of runoff in ungauged catchments. Hydrolog Sci J 59:1470-1490 doi:10.1080/02626667.2013.838003

Zhang D, Zhang L, Guan Y, Chen X, Chen X (2012) Sensitivity analysis of Xinanjiang rainfall–

runoff model parameters: a case study in Lianghui, Zhejiang province, China. Hydrol Res 43:123-134 doi:10.2166/nh.2011.131

Zhang H et al. (2019) Impacts of future climate change on water resource availability of eastern Australia: A case study of the Manning River basin. J Hydrol 573:49-59 doi:10.1016/j.jhydrol.2019.03.067

Zhao R-J (1992) The Xinanjiang model applied in China. J Hydrol 135:371-381 doi:10.1016/0022-1694(92)90096-E

Zhuo L, Han D, Dai Q, Islam T (2016) Chapter 15 - A Comparative Study on SMOS and NLDAS-2 Soil Moistures Over a Hydrological Basin—With Continental Climate. In: Srivastava PK, Petropoulos GP, Kerr YH (eds) Satellite Soil Moisture Retrieval. Elsevier, pp 289-308. doi:10.1016/B978-0-12-803388-3.00015-2

Figure

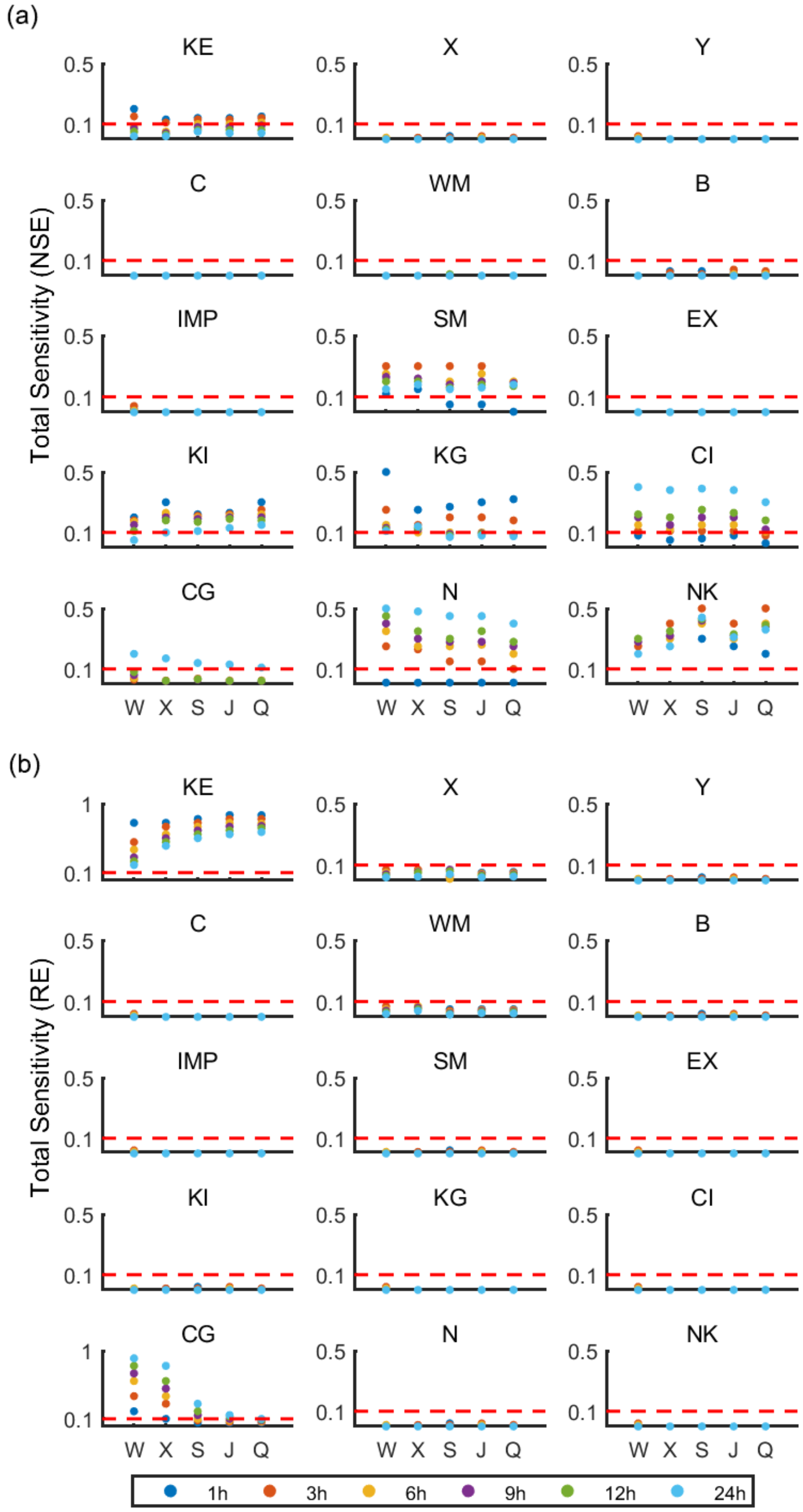

Fig. 1 Variation of parameter sensitivity with different temporal scales in five basins (W-Wuyishan; X-Xinchang; S-Shuiji; J-Jianyang; Q-Qilijie) with two different objective functions.

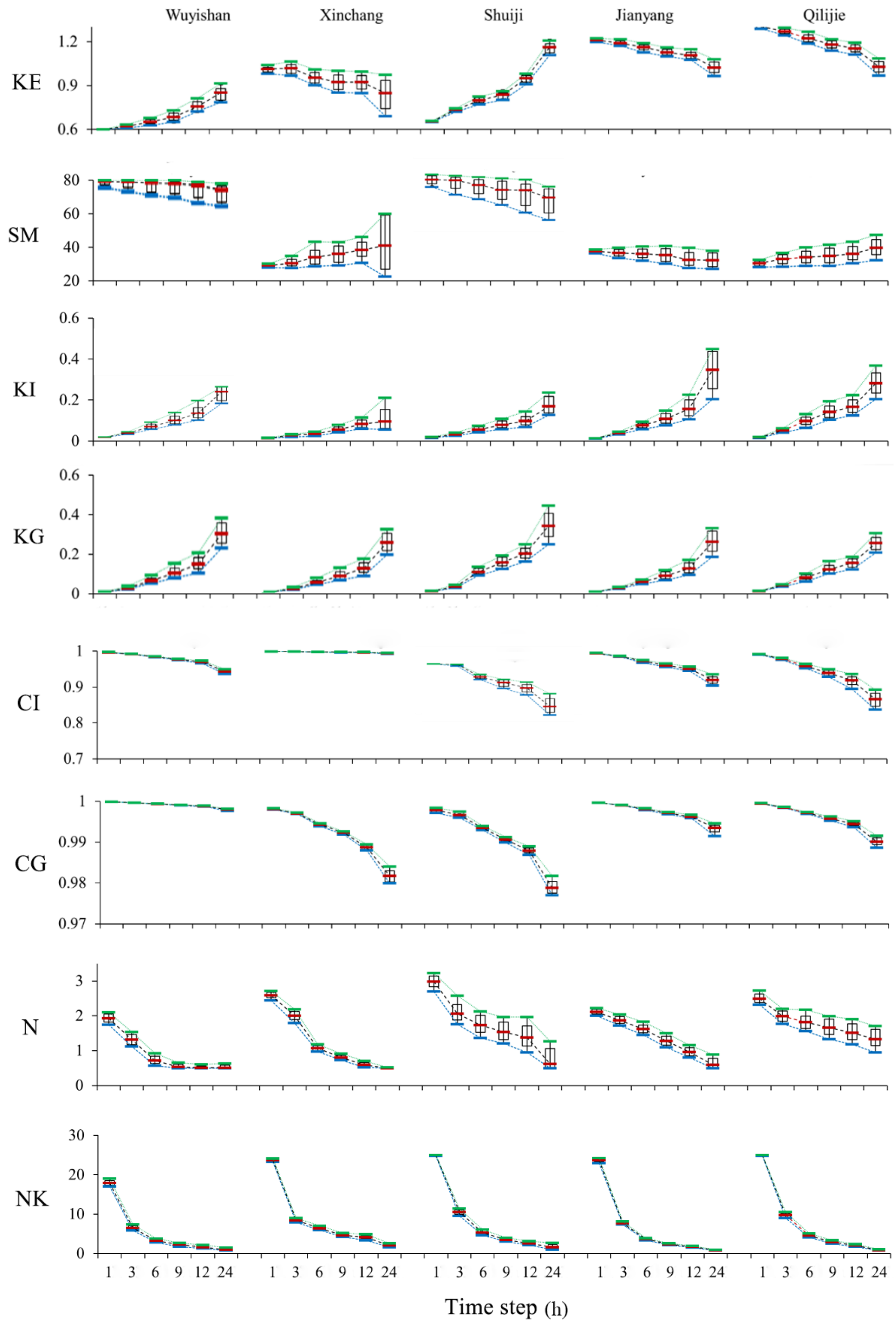

Fig. 2 Box plots of posterior distributions for sensitive flow routing parameters in each sub-basin with different temporal scales.

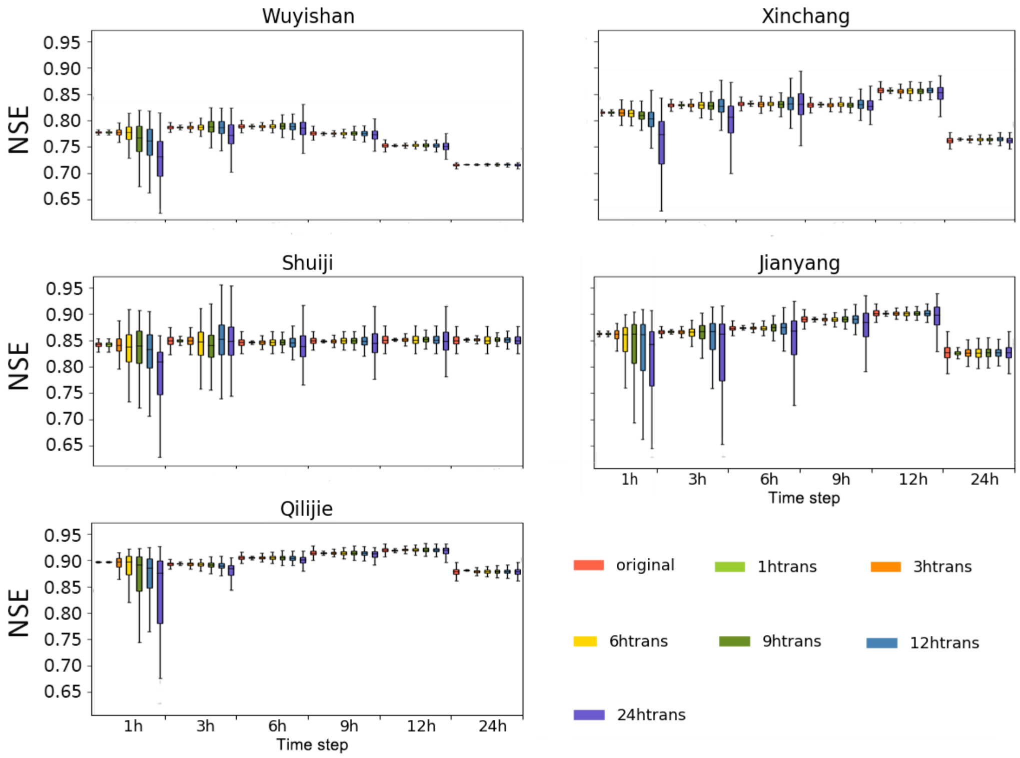

Fig. 3 Box plots of NSE values using parameters transferred from different temporal scales; color blocks from left to right represent 95% confidence intervals of NSE using parameters from calibration, at 1-, 3-, 6-, 9-, 12- and 24-hour time steps

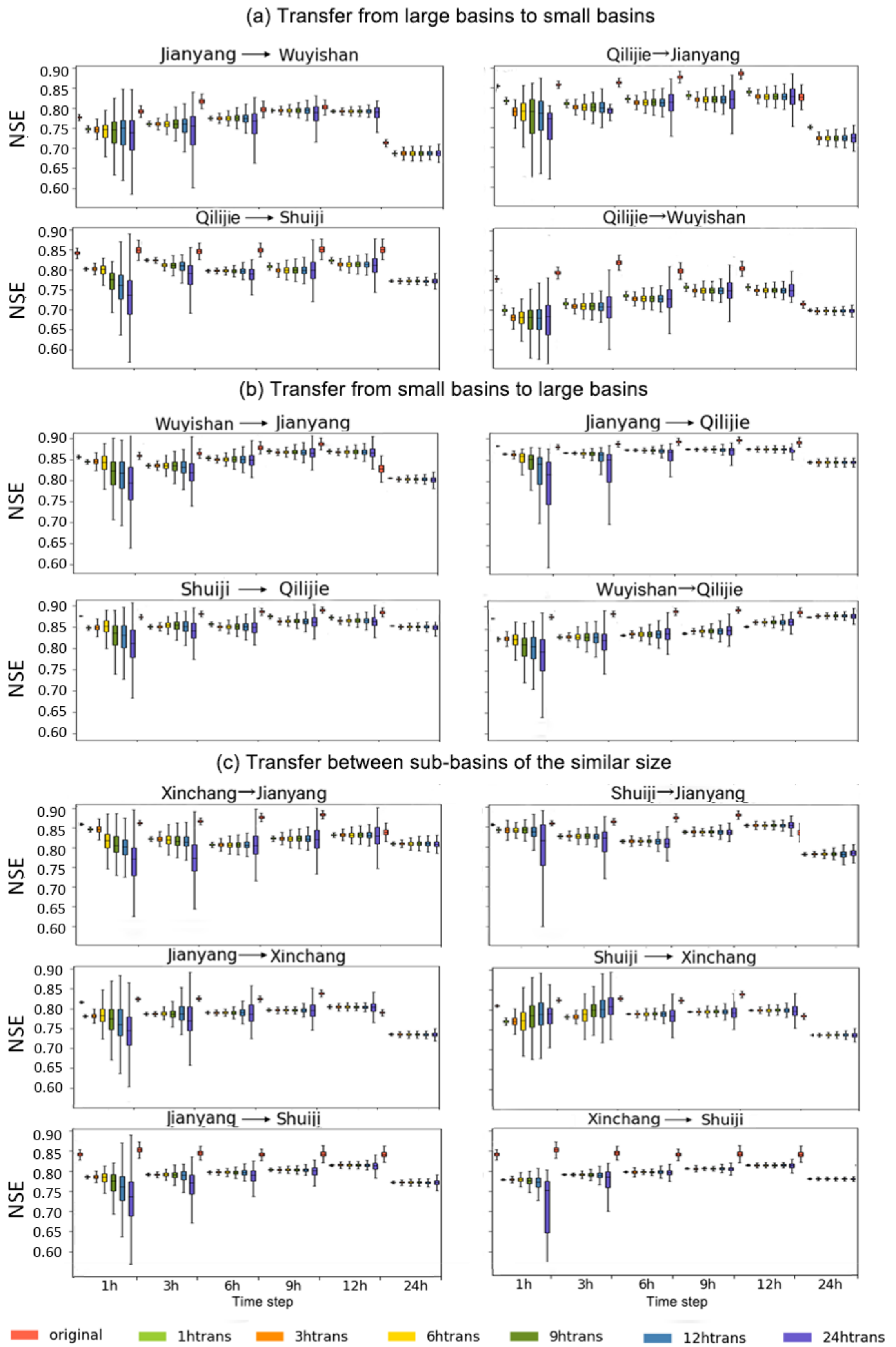

Fig. 4 Box plots of NSE values using parameters transferred from different temporal scales and basins. The directions of arrows in titles represent the direction of spatial

transfer. The first color block represents the 95% confidence interval of NSE using parameters from calibration, others from left to right represent parameters transferred from another basin at 1-, 3-, 6-, 9-, 12- and 24-hour time steps.

Table

Table 1 Characteristic data of Jianxi basin and its sub-basins

Basin	Wuyishan	Xinchang	Shuiji	Jianyang	Qilijie
Area (km^2)	1072	3060	3305	4837	14749
Rainfall runoff coefficient (-)	0.6261	0.6339	0.6476	0.5573	0.5447
Slope (°)	18.31	17.20	15.18	15.23	15.27
Farmland (%)	13.24	15.32	13.07	14.47	15.81
Forest (%)	82.17	79.66	81.52	80.22	78.75
Meadow (%)	3.25	3.63	3.88	3.82	3.95
Water body (%)	0.53	0.41	0.59	0.56	0.54
Bare land (%)	0.81	0.99	0.94	0.93	0.95

Table 2 Goodness-of-fits(R^2) of the temporal and spatial transfer functions for sensitive parameters

	Scale	P	W	X	S	J	Q	P	W	X	S	J	Q
Spatial	1h	KE	0.89	0.91	0.89	0.90	0.90	SM	0.91	0.93	0.91	0.92	0.92
	3h		0.88	0.90	0.88	0.89	0.89		0.91	0.92	0.90	0.92	0.91
	6h		0.88	0.90	0.88	0.89	0.89		0.90	0.92	0.90	0.91	0.91
	9h		0.86	0.88	0.86	0.87	0.87		0.88	0.90	0.88	0.90	0.89
	12h		0.88	0.89	0.88	0.89	0.89		0.90	0.92	0.90	0.91	0.91
	24h		0.88	0.90	0.88	0.89	0.89		0.90	0.92	0.90	0.91	0.91
	1h	KI	0.94	0.96	0.94	0.95	0.95	KG	0.94	0.96	0.94	0.95	0.95
	3h		0.93	0.95	0.93	0.95	0.94		0.93	0.95	0.93	0.95	0.94
	6h		0.93	0.95	0.93	0.94	0.94		0.93	0.95	0.93	0.94	0.94
	9h		0.91	0.93	0.91	0.93	0.92		0.91	0.93	0.91	0.92	0.92
	12h		0.93	0.95	0.93	0.94	0.94		0.93	0.95	0.93	0.94	0.94
	24h		0.93	0.95	0.93	0.94	0.94		0.93	0.95	0.93	0.94	0.94
	1h	CI	0.93	0.95	0.93	0.94	0.94	CG	0.92	0.93	0.92	0.93	0.93
	3h		0.92	0.94	0.92	0.93	0.93		0.91	0.93	0.91	0.92	0.92
	6h		0.92	0.94	0.92	0.93	0.93		0.91	0.92	0.91	0.92	0.92
	9h		0.90	0.92	0.90	0.91	0.91		0.90	0.91	0.90	0.90	0.90
	12h		0.92	0.94	0.92	0.93	0.93		0.90	0.92	0.90	0.92	0.91
	24h		0.92	0.94	0.92	0.93	0.93		0.91	0.93	0.91	0.92	0.92
	1h	N	0.96	0.98	0.96	0.97	0.97	NK	0.97	0.99	0.97	0.98	0.98
	3h		0.95	0.97	0.95	0.97	0.96		0.96	0.98	0.96	0.98	0.97
	6h		0.95	0.97	0.95	0.96	0.96		0.96	0.98	0.96	0.97	0.97
	9h		0.93	0.95	0.93	0.94	0.94		0.94	0.96	0.94	0.95	0.95
	12h		0.95	0.97	0.95	0.96	0.96		0.96	0.98	0.96	0.97	0.97
	24h		0.95	0.97	0.95	0.96	0.96		0.96	0.98	0.96	0.97	0.97
Temporal		KE	0.98	0.91	0.98	0.99	0.99	SM	0.99	0.95	0.93	0.92	0.95
		KI	0.99	0.99	0.99	0.99	0.98	KG	0.99	0.99	0.98	0.99	0.98
		CI	0.99	0.98	0.99	0.98	0.99	CG	0.99	0.99	0.99	0.99	0.99
		N	0.91	0.95	0.94	0.95	0.99	NK	0.99	0.98	0.99	0.99	0.99

(P-Parameter; W-Wuyishan; X-Xinchang; S-Shuiji; J-Jianyang; Q-Qilijie)

Table 2 Median_NSE and ARIL for three typical flood events transferred from different temporal scale and basin by using posterior distribution parameters.

		W_6	J_1-W_6	Q_1-W_6	Q_6	J_1-Q_6	W_1-J_6	J_6	X_1-J_6	S_1-J_6
P=80%	NSE(Median)	0.75	0.74	0.74	0.82	0.79	0.78	0.75	0.75	0.75
	ARIL(95%)	1.52	1.18	1.18	1.31	1.29	1.29	1.18	1.17	1.17
P=50%	NSE(Median)	0.88	0.88	0.88	0.88	0.86	0.86	0.90	0.90	0.90
	ARIL(95%)	0.94	0.85	0.85	1.03	1.03	1.03	1.02	1.02	1.02
P=5%	NSE(Median)	0.95	0.92	0.92	0.98	0.98	0.98	0.95	0.95	0.95
	ARIL(95%)	0.88	0.83	0.83	0.99	0.99	0.99	1.00	0.99	0.99

Note: W-Wuyishan; J-Jianyang; Q-Qilijie; S-Shuiji; X-Xinchang; J_1-W_6: simulation in Wuyishan at 6-hour using parameters transferred from Jianyang at 1-hour, ect. P is the flood frequency.

Supplementary material

Table S1 Description and range of Xinanjiang model parameters

Classification	Parameter	Physical meaning	Range	Unit
Evapotranspiration	KE	Ratio of potential evapotranspiration to pan evaporation	0.6-1.3	-
	X	the coefficient of the upper layer tension water storage capacity	01-0.6	-
	Y	the coefficient of the lower layer tension water storage capacity	0.1-0.6	-
	C	Evapotranspiration coefficient of deep layer	0.15-0.2	-
Runoff production	WM	Areal mean tension water storage capacity	100-200	mm
	B	Exponent of the tension water-capacity distribution curve	0.1-0.8	-
	IMP	Factor of impervious area	0.01-0.1	-
Runoff separation	SM	Free water-storage capacity	10-80	mm
	EX	Exponential of distribution of free water-storage capacity	1.0-1.5	-
	KI	Out flow coefficient of free water storage to interflow	0.01-0.45	-
	KG	Out flow coefficient of free water storage to groundwater flow	0.01-0.45	-
Flow routing	CI	Recession constant of lower-interflow storage	0.7-1	-
	CG	Recession constant of groundwater storage	0.97-1	-
	N	Parameter of Nash unit hydrograph (Number of linear reservoirs)	0.5-12	-
	NK	Parameter of Nash unit hydrograph (Concentration time)	0.8-25	-

Table S2 Coefficients of the temporal and spatial transfer functions for sensitive evapotranspiration parameter

Parameter	Transfer	Scale	$10^5*\mu 1$	$\mu 2$	W	X	S	J	Q
					*10*μ0*				
KE	Spatial	1h	1.27	-4.68	-1.88	2.36	-0.63	0.53	-0.39
		3h	1.38	-3.77	-1.95	2.04	-0.31	0.63	-0.42
		6h	1.28	-3.24	-1.72	1.29	0.16	0.67	-0.40
		9h	1.18	-2.71	-1.50	0.87	0.35	0.64	-0.36
		12h	1.28	-1.58	-1.29	0.26	0.71	0.65	-0.33
		24h	1.24	0.68	-0.94	-1.26	1.75	0.78	-0.32
	Temporal		-		*10*K*				
					0.11	-0.07	0.22	-0.08	-0.12

(W-Wuyishan; X-Xinchang; S-Shuiji; J-Jianyang; Q-Qilijie)

Table S3 Coefficients of the temporal and spatial transfer functions for sensitive runoff separation parameter

Parameter	Transfer	Scale	*10^5*μ1*	*μ2*	W	X	S	J	Q
							*10*μ0*		
SM	Spatial	1h	-114.75	222.5	184.6	-311.2	128.1	-35.6	34.1
		3h	-81.96	241.1	187.8	-300.9	117.1	-39.5	35.5
		6h	-77.23	232.8	185.3	-260.1	84.6	-46.6	36.8
		9h	-76.32	219.2	191.2	-230.5	55.5	-56.0	39.9
		12h	-30.94	269.5	191.5	-212.5	40.1	-59.9	40.8
		24h	-30.94	269.5	191.5	-212.5	40.1	-59.9	40.8
	Temporal		-				*K*		
					-0.14	0.53	-0.64	-0.24	0.37
KI	Spatial	1h	0.01	0.03	0.06	-0.04	-0.01	-0.02	0.01
		3h	-0.01	-0.11	0.18	-0.10	-0.04	-0.08	0.04
		6h	-0.10	-0.37	0.41	-0.30	-0.04	-0.16	0.10
		9h	-0.15	-0.53	0.62	-0.41	-0.11	-0.25	0.15
		12h	-0.54	-0.91	0.78	-0.46	-0.18	-0.33	0.19
		24h	-1.82	-2.82	1.37	-1.17	-0.01	-0.50	0.31
	Temporal		-				*K*		
					0.07	0.04	0.07	0.13	0.11
KG	Spatial	1h	0.04	0.03	0.00	-0.01	0.01	0.00	0.00
		3h	0.15	0.07	-0.02	-0.02	0.03	0.01	-0.01
		6h	0.43	0.41	-0.09	-0.28	0.31	0.11	-0.04
		9h	0.59	0.49	-0.06	-0.52	0.48	0.14	-0.04
		12h	0.56	0.44	-0.07	-0.68	0.62	0.18	-0.05
		24h	0.56	0.44	-0.07	-0.68	0.62	0.18	-0.05
	Temporal		-				*K*		
					0.10	0.09	0.13	0.11	0.11

(W-Wuyishan; X-Xinchang; S-Shuiji; J-Jianyang; Q-Qilijie)

Table S4 Coefficients of the temporal and spatial transfer functions for sensitive flow routing parameters

Parameter	Transfer	Scale	*10^5*μ1*	*μ2*	W	X	S	J	Q
					*10*μ0*				
CI	Spatial	1h	-0.02	0.05	-0.01	0.01	0.00	0.00	0.00
		3h	-0.03	0.13	-0.03	0.03	0.00	0.01	-0.01
		6h	-0.30	-0.24	0.07	0.29	-0.29	-0.10	0.03
		9h	-0.45	-0.35	0.10	0.42	-0.42	-0.14	0.05
		12h	-0.62	-0.48	0.11	0.54	-0.53	-0.17	0.06
		24h	-1.05	-0.90	0.17	0.95	-0.92	-0.29	0.09
	Temporal		-		*10*K*				
					-0.02	-0.01	-0.08	-0.03	-0.06
CG	Spatial	1h	-0.01	-0.02	0.01	0.00	0.00	0.00	0.00
		3h	-0.02	-0.03	0.01	-0.01	-0.01	-0.01	0.00
		6h	-0.04	-0.06	0.03	-0.01	-0.01	-0.01	0.01
		9h	-0.05	-0.08	0.04	-0.01	-0.02	-0.02	0.01
		12h	-0.07	-0.11	0.05	-0.03	-0.02	-0.02	0.01
		24h	-0.07	-0.11	0.05	-0.03	-0.02	-0.02	0.01
	Temporal		-		*100*K*				
					-0.02	-0.07	-0.08	-0.03	-0.04
N	Spatial	1h	8.24	10.49	-3.89	0.30	2.57	2.05	-1.03
		3h	4.59	3.18	-4.14	1.63	1.63	1.91	-1.03
		6h	5.89	0.13	-4.20	-1.88	4.63	2.67	-1.22
		9h	7.47	1.68	-3.45	-2.35	4.48	2.36	-1.04
		12h	8.42	3.53	-1.99	-3.07	4.02	1.72	-0.68
		24h	7.11	1.06	0.79	-0.78	0.08	-0.27	0.17
	Temporal		-		*β*				
					-0.48	-0.57	-0.42	-0.41	-0.20
NK	Spatial	1h	43.77	21.25	-37.26	9.83	18.73	18.20	-9.50
		3h	36.38	33.02	-12.73	-3.78	12.40	7.70	-3.60
		6h	19.53	28.61	-12.28	13.29	-2.29	3.91	-2.64
		9h	11.77	20.45	-8.73	12.01	-3.79	2.24	-1.75
		12h	8.94	18.36	-8.55	13.39	-5.07	1.87	-1.63
		24h	8.94	18.36	-8.55	13.39	-5.07	1.87	-1.63
	Temporal		-		*β*				
					-0.93	-0.83	-0.90	-1.05	-1.05

(W-Wuyishan; X-Xinchang; S-Shuiji; J-Jianyang; Q-Qilijie)

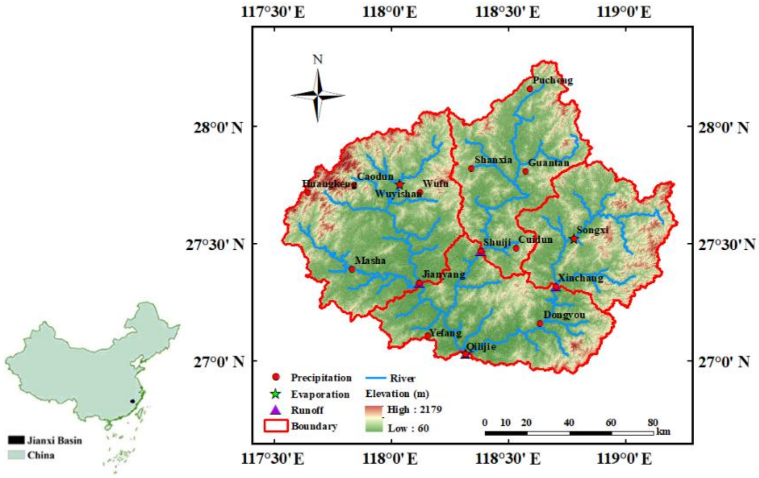

Fig. S1 Geographical distribution of hydrological stations and sub-basins in Jianxi basin.

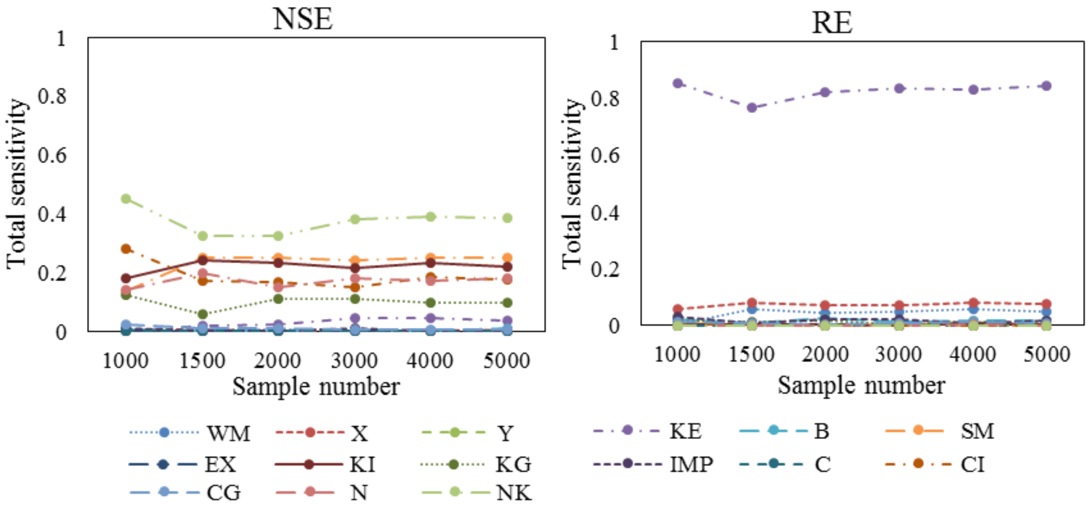

Fig. S2 Total sensitivity of each parameter with different sampling numbers using two different objective functions when the temporal scale is 1 h.

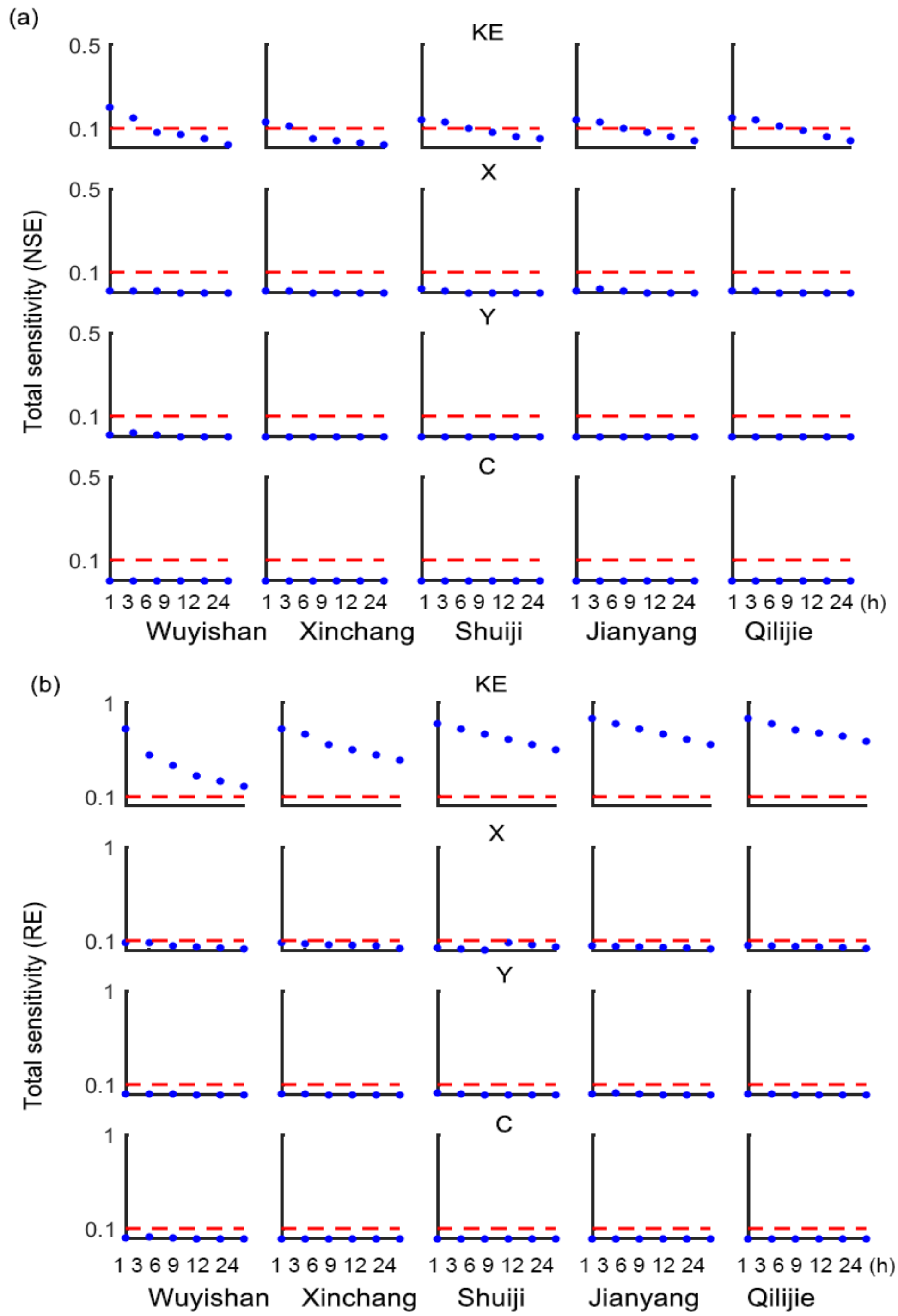

Fig. S3 Variation of evapotranspiration parameter sensitivity with different temporal scales with two different objective functions.

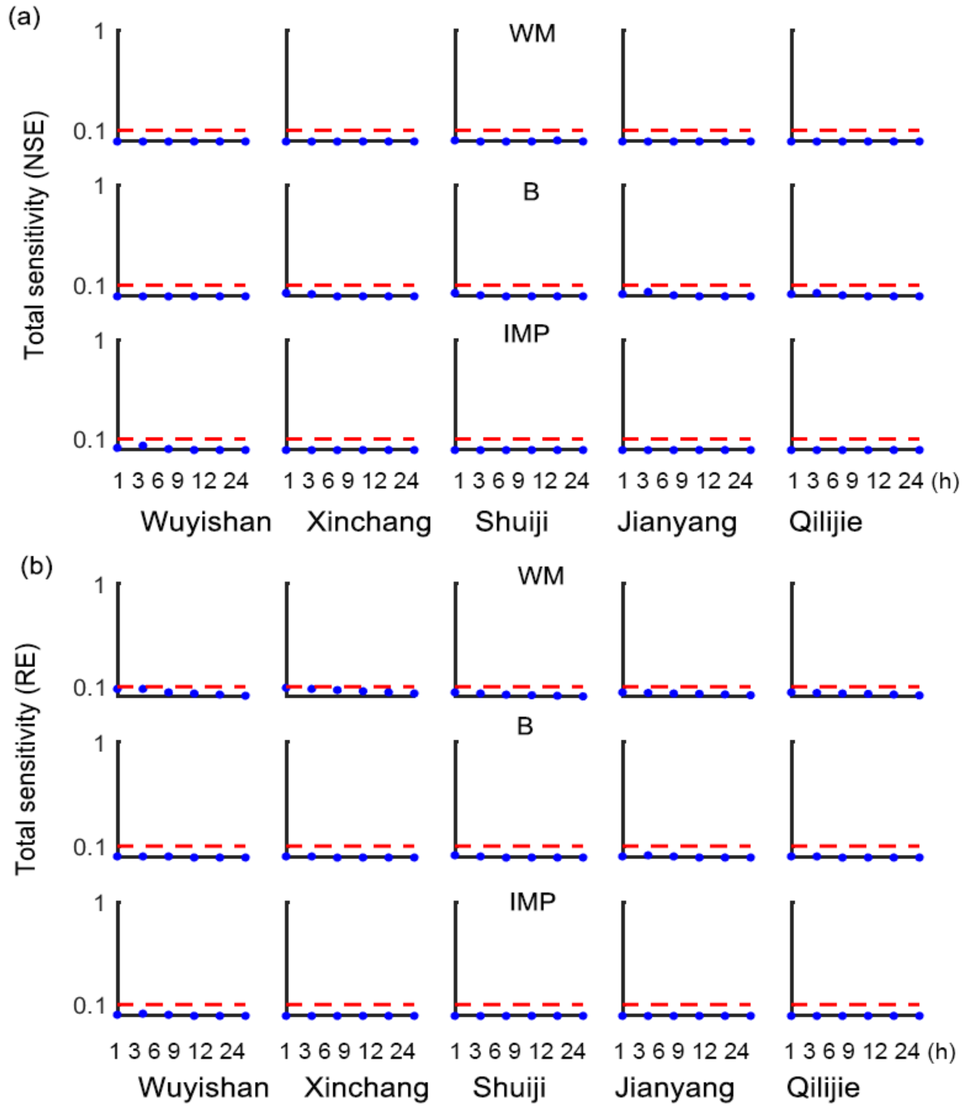

Fig. S4 Variation of runoff production parameter sensitivity with different temporal scales with two different objective functions.

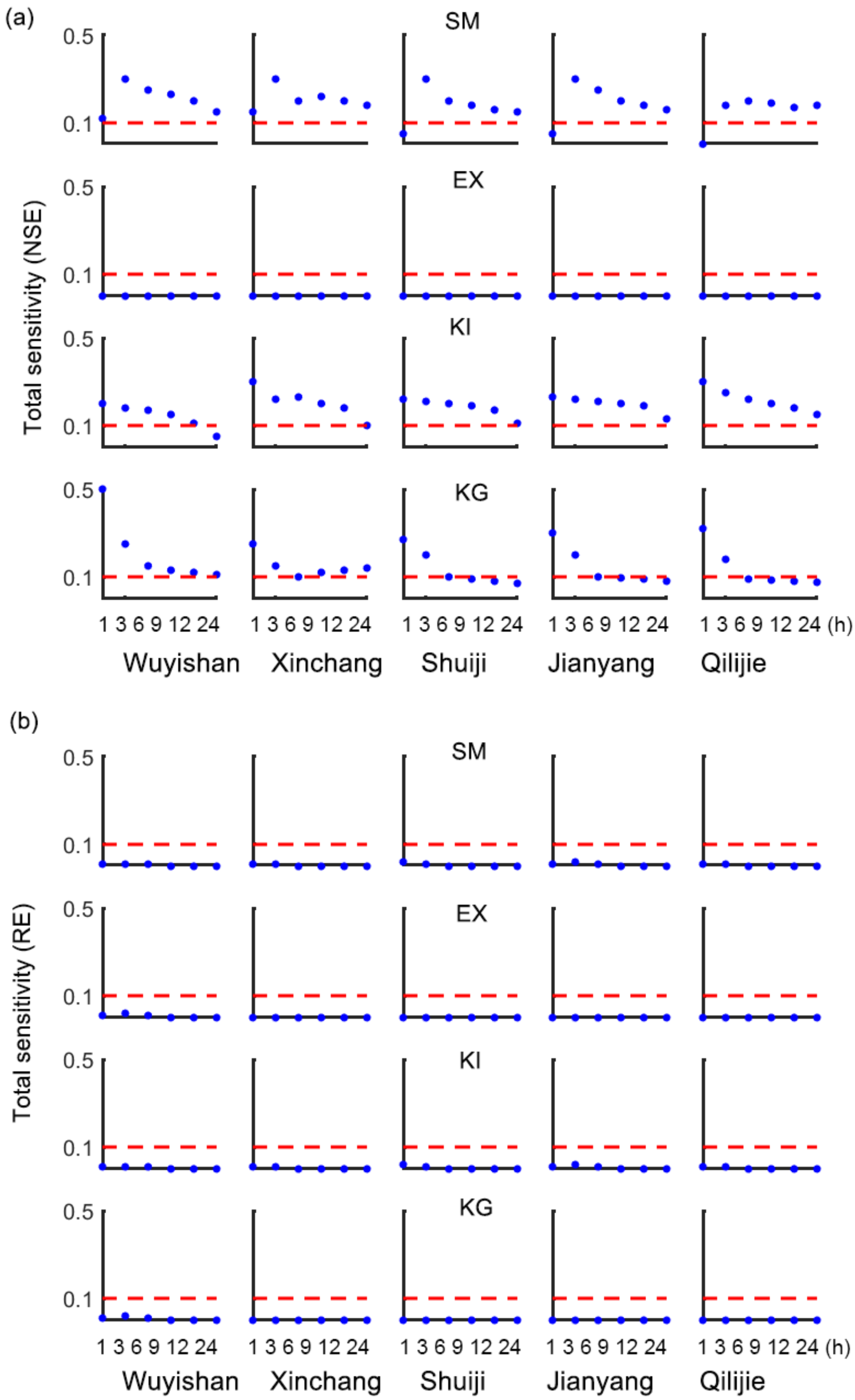

Fig. S5 Variation of runoff separation parameter sensitivity with different temporal scales with two different objective functions.

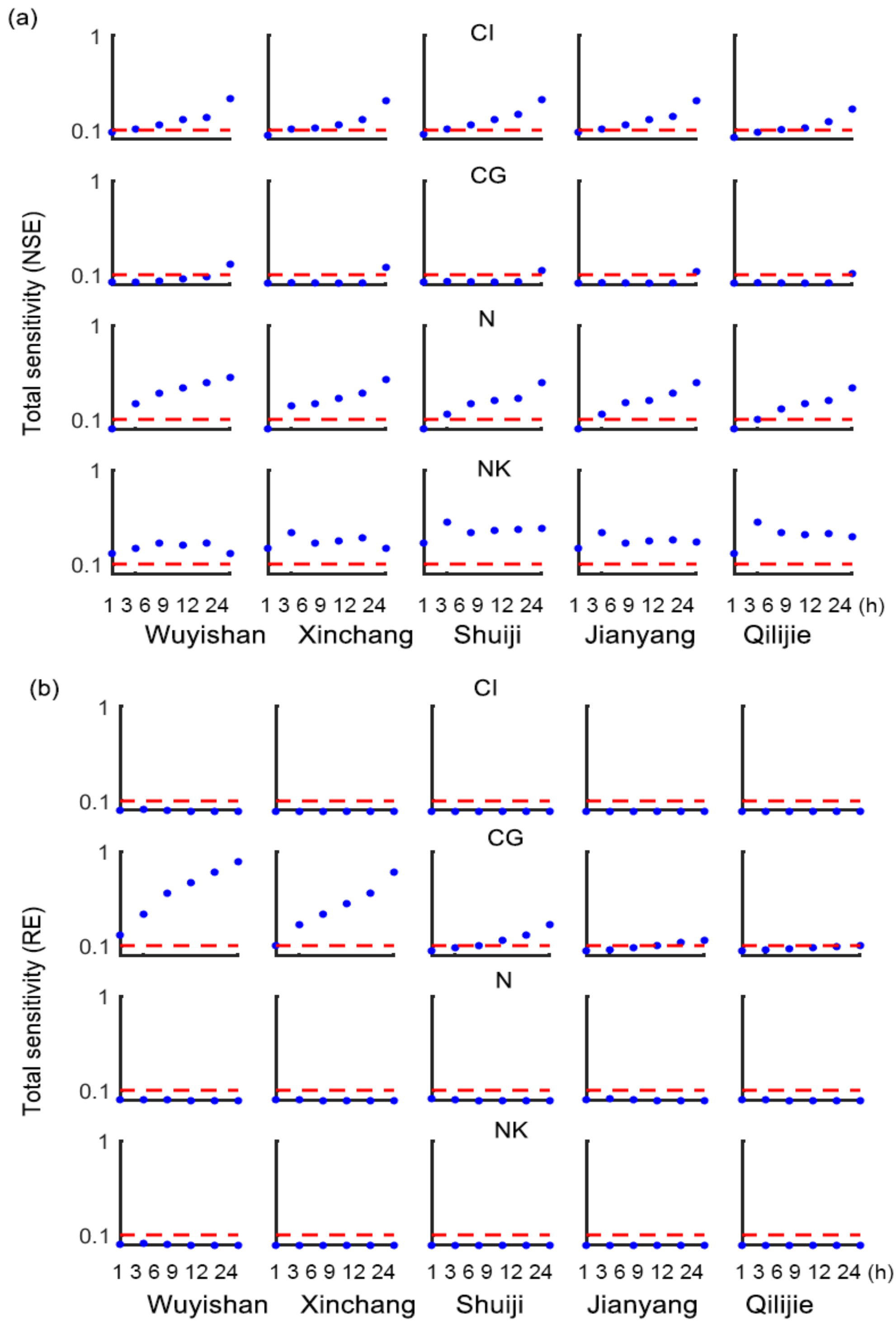

Fig. S6 Variation of flow routing parameter sensitivity with different temporal scales with two different objective functions.

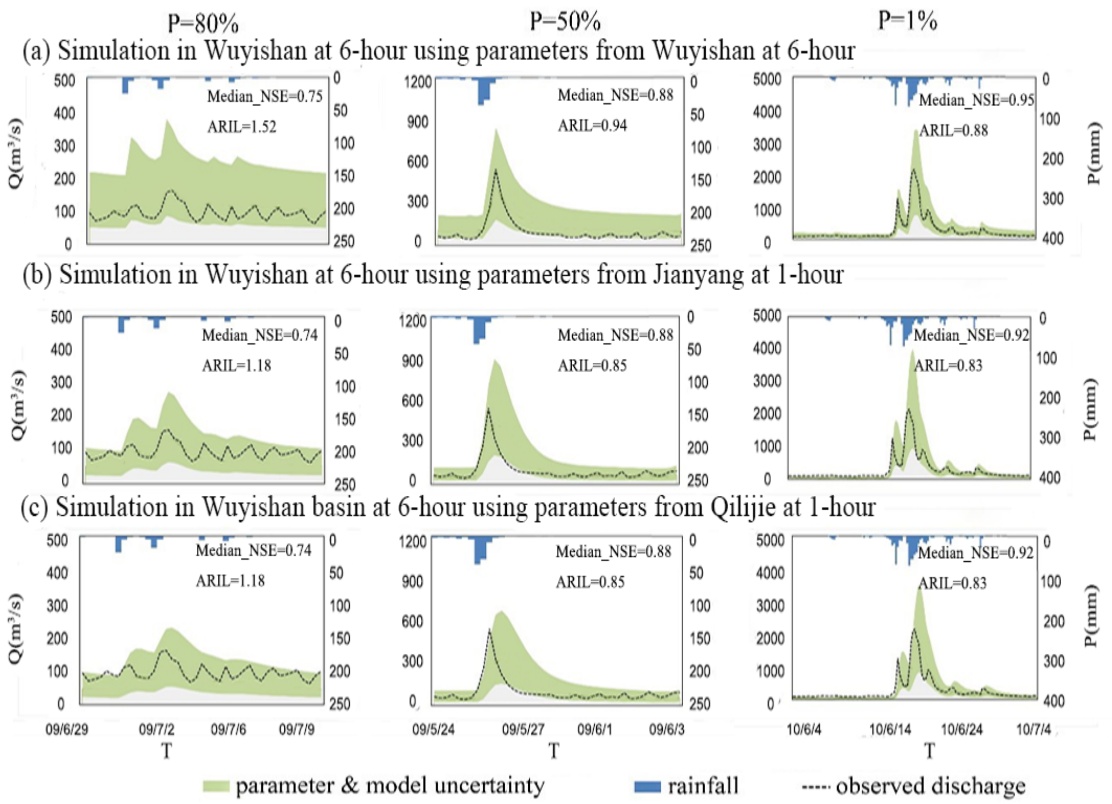

Fig. S7 95% confidence intervals of simulated runoff processes for three typical flood events at a 6-hour temporal scale using posterior distribution parameters, and parameters transferred from a 1-hour temporal scale and from a large basin to a small basin. The light-green shadowed regions represent 95% confidence intervals of both parameter and model uncertainty.

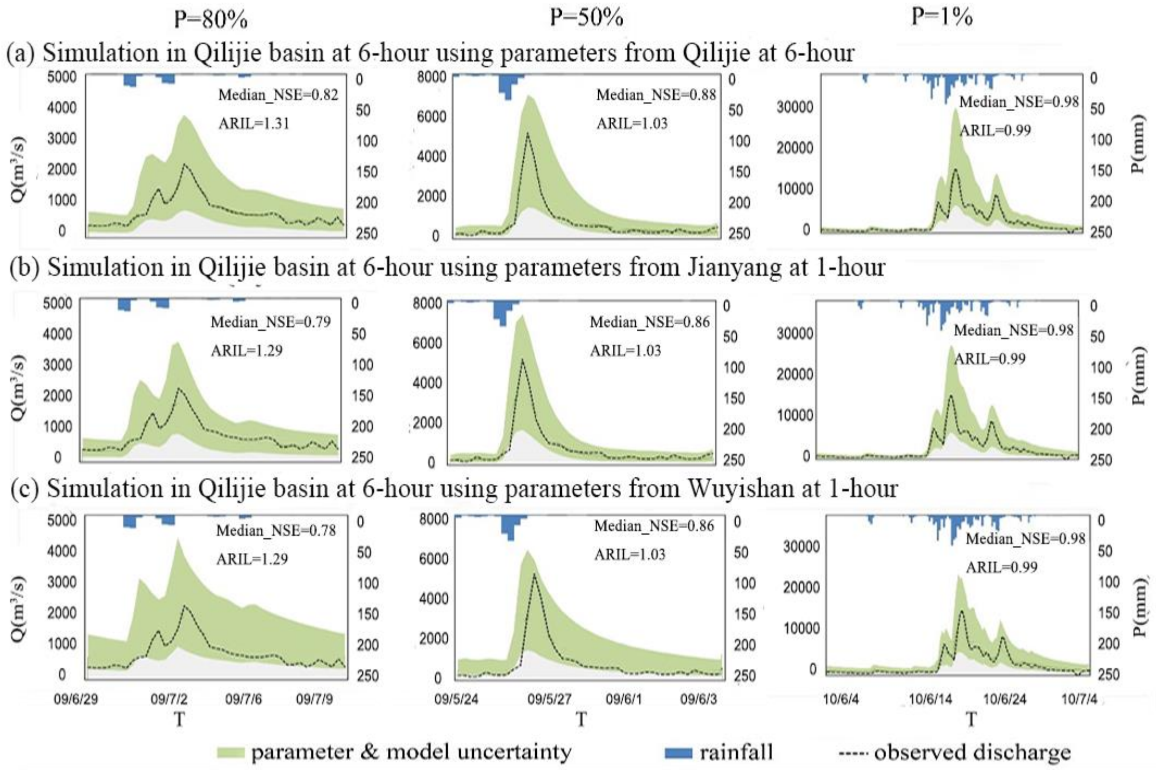

Fig. S8 95% confidence intervals of simulated runoff processes for three typical flood events at a 6-hour temporal scale using posterior distribution parameters, with parameters transferred from a 1-hour temporal scale and from a small basin to a large basin. The light-green shadowed regions represent 95% confidence intervals of both parameter and model uncertainty.

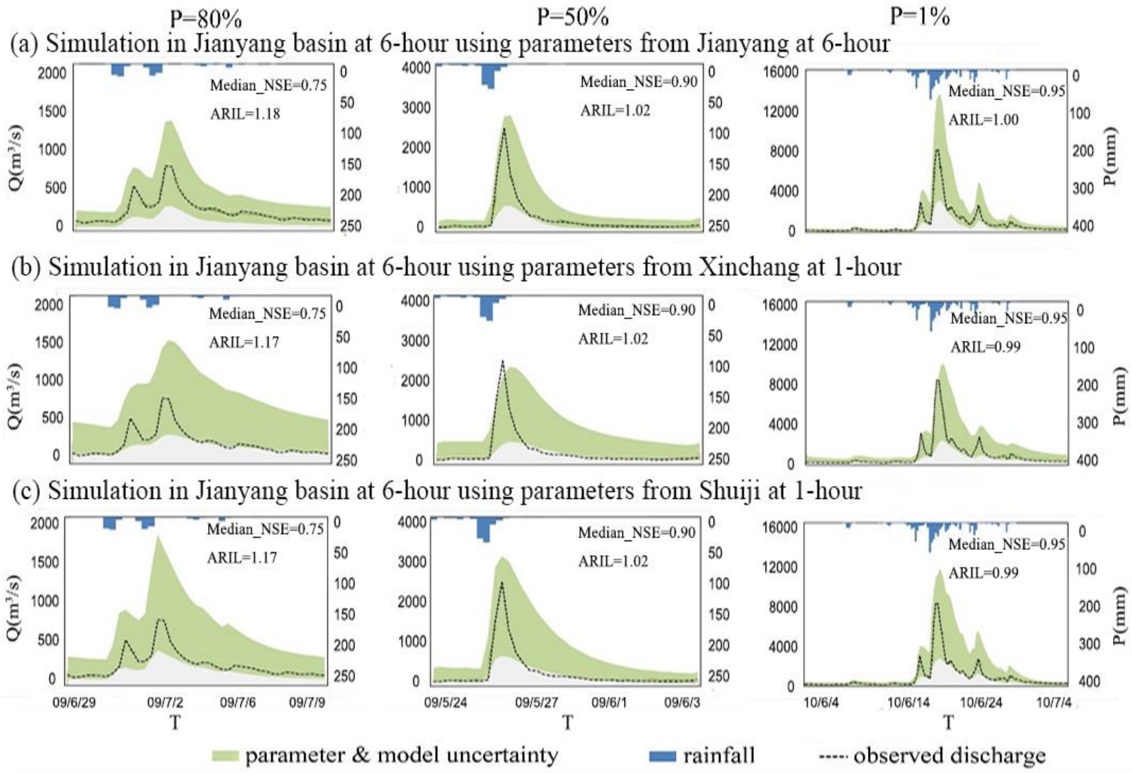

Fig. S9 95% confidence intervals of simulated runoff processes for three typical flood events at a 6-hour temporal scale using posterior distribution parameters, with parameters transferred from a 1-hour temporal scale and a similarly sized basin. The light-green shadowed regions represent 95% confidence intervals of both parameter and model uncertainty.